2021 IEEE/ASME International Conference on
Advanced Intelligent Mechatronics (AIM)

A Magnetically-Steerable Stenting Catheter for Minimally Invasive Cardiovascular Interventions

Venkatasubramanian Kalpathy Venkiteswaran[1*], Jesus Jimenez Palao[1], and Sarthak Misra[1,2]

***Abstract*— Magnetically-guided catheters present a promising treatment option to reduce the incidence of post-operative trauma in minimally invasive procedures. In this study, we present a novel catheter design that combines the characteristics of standard angiography and angioplasty catheters in combination with magnetic guidance. The catheter body consists of a 5F size angiography catheter that has been adapted to hold an intra-aortic balloon (8F diameter). It uses two magnets, one for tip guidance and another for easy steering into blood vessel branches. Magnetic guidance of the catheter is demonstrated using an array of six mobile electromagnetic coils with a custom-built graphical user interface. A 3R pseudo-rigid-body model is used within a closed-loop controller to calculate the coil currents and positions to obtain the required magnetic field in order to control the orientation of the catheter tip. Magnetic guidance of the catheter is demonstrated in a phantom model of the aorta. The angiography and angioplasty capabilities of the catheter are illustrated through separate experiments.**

I. Introduction

Cardiovascular diseases are the leading cause of death for both men and women worldwide, with ischemic heart disease and stroke accounting for more than 15 million deaths worldwide each year [1]. These types of diseases are predominantly caused by stenosis (narrowing) of blood vessels leading to ischemia (lack of oxygen) or hemorrhage in major organs such as the heart or the brain. Besides cardiovascular stenotic lesions, abdominal aortic aneurysm (AAA) is a very common case of this type of disease, affecting mainly elderly men. The disease presents itself as an inflamed zone in the aorta. Due to the stress generated by the inflammation, the zone becomes weak, which in turn puts patients at great risk of arterial rupture (ruptures from large AAA have an approximate 90% mortality rate) [2].

Minimally invasive surgery (MIS), due to its positive patient outcomes (fewer post-surgery complications, faster mobilization), is currently used to treat many cases of cardiovascular disease [3]. However, technical challenges with MIS limit its application to simpler, less-challenging cases, in spite of the its benefits for both patients and hospitals [4]. Endovascular aortic repair (EVAR), the current MIS procedure to mitigate the symptoms of AAA, has been shown to be successful in the short term, but due to the nature of this procedure many complications such as endoleaks, endograft migration or collapse, stenosis, graft infection and end-organ ischemia may appear for a significant group of patients (between 16% and 30% of the cases) [5], resulting in the undesirable scenario of the patient having to undergo additional operations. By improving the tools available for MIS, it is possible to push the boundaries of current surgical procedures and stimulate its use for challenging operations.

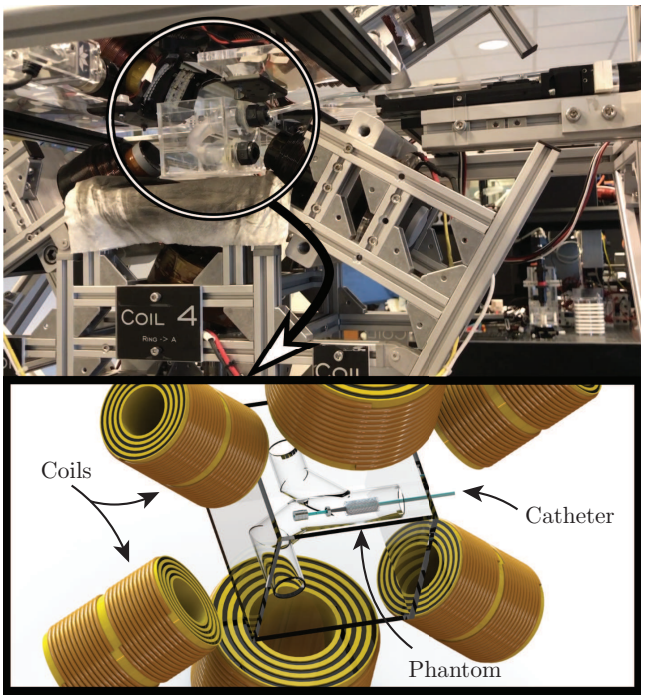

Fig. 1: (Top) Array of six mobile electromagnetic coils (BigMag) used for testing magnetic stenting catheter. A phantom of the aorta is prototyped and placed in the setup. (Bottom) Illustration of test setup with magnetic catheter inside the transparent phantom.

Remote magnetic navigation (RMN) is a recent technological development that allows wireless control of MIS catheters using magnetic fields, with benefits such as overcoming vascular obstructions and easier chamber access [6]. Control using magnetic fields also provides greater catheter stability, and enhances safety due to reduced contact force, thereby preventing perforation [7]. Currently, RMN has found application primarily in ablation procedures [8], [9], with commercial systems now on the market (e.g., Niobe, Stereotaxis Inc., St. Louis, USA).

[1]Surgical Robotics Laboratory, Department of Biomechanical Engineering, University of Twente, 7500 AE Enschede, The Netherlands.
[2]Department of Biomedical Engineering, University of Groningen 9713 GZ Groningen, The Netherlands.
*E-mail v.kalpathyvenkiteswaran@utwente.nl
This research has received funding from the Pioneers in Healthcare Innovation fund supported by University of Twente, Saxion University, Medisch Spectrum Twente, Ziekenhuis Groep Twente and Deventer Hospital under the project MADSC (Magnetically-Actuated Deployable Stent Catheter for Percutaneous coronary Interventions). It has also received funding from the Crazy Research Call from the Faculty of Engineering Technology at the University of Twente under the project 'Symbiobot'.

Due to the potential impact of RMN, magnetic actuation of MIS devices has generated significant interest in the field of surgical robotics [10]. In general, the MIS devices have either active electromagnetic coils or passive permanent magnets on board, which are controlled using external magnetic field developed by an actuation unit. Liu *et al.* developed a catheter with multiple coils that is compatible with magnetic resonance imaging (MRI) [11]. Sikorski *et al.* used a combination of an embedded electromagnetic coil and a permanent magnet to achieve grasping function [12]. Magnetic steering of passive guidewires has been explored with the aim of improving steering precision and reducing trauma due to catheter contact [13], [14]. Pre-clinical trials of steering using an MRI scanner, and in combination with microultrasound have also been demonstrated [15], [16].

In this paper, we present a design for a magnetic catheter for stenting applications. The design combines the attributes of commonly used angiography (visualization of blood vessels) and angioplasty (widening of stenosis) catheters into one, with the added benefit of being steered by magnetic fields. It is developed specifically with the idea of addressing challenging procedures such as EVAR, in cases of AAA when multiple stents must be placed in different branches of the aorta. Currently, this is done using multiple stenting catheters introduced through different blood vessels, but we demonstrate an approach to achieve this with a single magnetically-controlled catheter. The magnetic steering follows a simplified control logic based on a kinematic model, and is demonstrated using an existing magnetic actuation system [17]. The capabilities of the catheter to deliver angiographic dye and place a stent within a vessel wall are demonstrated as through laboratory experiments. It is expected that by using a multi-functional catheter, not only can the performance of the current magnetically actuated operations be improved, but the total radiation exposure for both patients and physicians during angiography can be reduced.

II. Design of Magnetic Stenting Catheter

The catheter design developed in this work has four major requirements:

- It must be capable of being steered using magnetic fields, with stable motion of the catheter tip during steering and stenting.
- It can fit different stents so that multiple successive angioplasties can be performed with one catheter.
- It should be able to deliver a dye for imaging purposes.
- It can perform the above tasks within the vessel architecture of the aorta, for AAA treatment.

The magnetic stenting catheter is designed with consideration to the above requirements. The final design is shown in Fig. 2. It consists of a hollow inner channel that acts similar to a guidewire, with two sets of magnets near its tip. The hollow channel can carry fluoroscopic dye, and disperse it through holes between the two magnets. The magnet at the distal tip is stronger, and serves to deflect the catheter tip under the influence of the external magnetic field. The more proximal magnet is weaker in strength, and helps to achieve a more continuous, softer bend of the catheter tip. If only the distal magnet is included, the catheter tip undergoes sharp bends, which makes steering around bends more challenging. The second magnet is particularly useful to prevent the catheter tip pushing against the vessel wall and risking perforation.

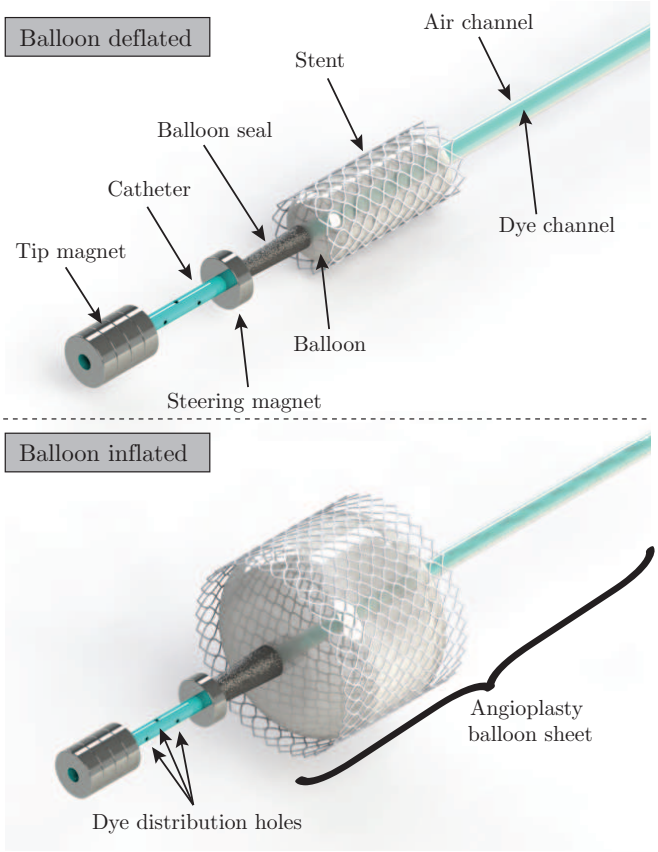

Fig. 2: Illustration of the catheter prototype in its deflated and inflated form. The catheter body (light blue) performs the functions of a standard angiography catheter using its main body to deliver the contrast solution to the tip of the catheter were the distribution holes are located. The catheter body also serves as a guidewire for different sizes of angioplasty sheaths that contain a pre-placed stent.

Outside the inner channel, a sheath with an angioplasty balloon is designed with a vacuum seal at its tip. The sheath is retractable, so that multiple stents may be placed following one another during angioplasty. During the procedure, the inner tube is inserted first, steered by the magnets while being aided by fluoroscopic dye, and guided to the target angioplasty site. The sheath with the balloon and stent is then inserted over the inner channel and the vacuum seal locks into place behind the second magnet. The stent is then deployed by inflating the balloon, following which the sheath can be retrieved and the catheter repositioned for a second stent. Through this design, it is possible to perform multiple angioplasties in adjacent blood vessels without the need for multiple insertions and removals of catheters, thereby reducing the angiographic imaging requirements and thus reducing X-ray exposure.

A prototype of the magnetic stenting catheter was fabricated using a 6F catheter (2mm outer diameter). Ring magnets of

6mm outer diameter and 2mm inner diameter were fixed onto the catheter (N45, Webcraft GmbH, Germany). The vacuum seal for the balloon sheath was 3D printed using stereolithography (SLA). The balloon from a Foley catheter was attached to the vacuum seal to make the outer sheath to demonstrate the angioplasty function. The catheter was less that 10mm in outer diameter in the uninflated case. The abdominal aorta is about 30mm in diameter, so these dimensions are acceptable for AAA treatment.

In the next section, a kinematic model is used to calculate the magnetic field necessary to steer the catheter during insertion.

III. Pseudo-Rigid-Body Model

In this section, a description and the mathematical equations of the 3R PRB (Pseudo-Rigid-Body) model used to estimate the necessary magnetic field for a desired catheter tip bending angle are presented . In this approach, the catheter stem is modeled as a flexible beam and discretized into rigid links and revolute joints [18]. By transforming the differential equations that define a the behavior of a flexible beam into algebraic kinematic equations for rigid bodies, the computational time is significantly reduced, allowing for real-time implementation of the forward model. The equations are directly adapted from the 3R PRB model by Venkiteswaran and Su [19] for flexible beams of uniform cross section.

As seen in Fig. 3, the PRB model consists of $n+1$ number of rigid links, with n revolute joints between them. Each joint has a torsional spring stiffness K_i, the length of each link is $l\gamma_i$, where l is the total length of the flexible beam and γ_i is the length ratio of each link, constrained by

$$\gamma_0 + \gamma_1 + \gamma_2 + \gamma_3 = 0. \tag{1}$$

If θ_i is the deflection of revolute joint i, the angular deflection of the tip of the PRB model is given by

$$\theta_T = \theta_1 + \theta_2 + \theta_3, \tag{2}$$

and the coordinates of the tip are given by

$$\begin{aligned} X_T = l(&\gamma_0 + \gamma_1 \cos(\theta_1) + \gamma_2 \cos(\theta_1 + \theta_2) \\ &+ \gamma_3 \cos(\theta_1 + \theta_2 + \theta_3)), \end{aligned} \tag{3}$$

$$\begin{aligned} Y_T = l(&\gamma_0 + \gamma_1 \sin(\theta_1) + \gamma_2 \sin(\theta_1 + \theta_2) \\ &+ \gamma_3 \sin(\theta_1 + \theta_2 + \theta_3)). \end{aligned} \tag{4}$$

The angular deflection associated with link $i = 0$ (θ_0) is assumed to be zero since the base of the beam is rigidly fixed. The magnetic torque being applied on the magnetic tip of the catheter is obtained by using Eq. 5, where τ is a vector containing the internal torques being exerted at each of the PRB joints. J^T is the transpose of the catheter Jacobian (obtained by differentiating the kinematic equations of the body) and W is the external loads being applied on the catheter's tip.

$$\tau = J^T W. \tag{5}$$

Assuming no mechanical forces are being applied on the catheter, and the deformation is caused solely by the magnetic field acting on the catheter's tip, the external loads vector is defined as

$$W = \begin{bmatrix} 0 & 0 & M \end{bmatrix}^T, \tag{6}$$

where M is the torque generated on the steering magnet by the magnetic field. Assuming the spring torques are proportional to the PRB model angles, the following expression can also be derived for the internal torques.

$$\tau = \begin{bmatrix} K_1\theta_1 & K_2\theta_2 & K_3\theta_3 \end{bmatrix}^T. \tag{7}$$

For the simplified loading case analyzed here, Eqn. 5 reduces to

$$\begin{bmatrix} K_1\theta_1 \\ K_2\theta_2 \\ K_3\theta_3 \end{bmatrix} = \begin{bmatrix} M \\ M \\ M \end{bmatrix}. \tag{8}$$

The values for K_i are determined experimentally through calibration experiments [18]. The magnetic torque (M) is calculated as described in Section IV-B.

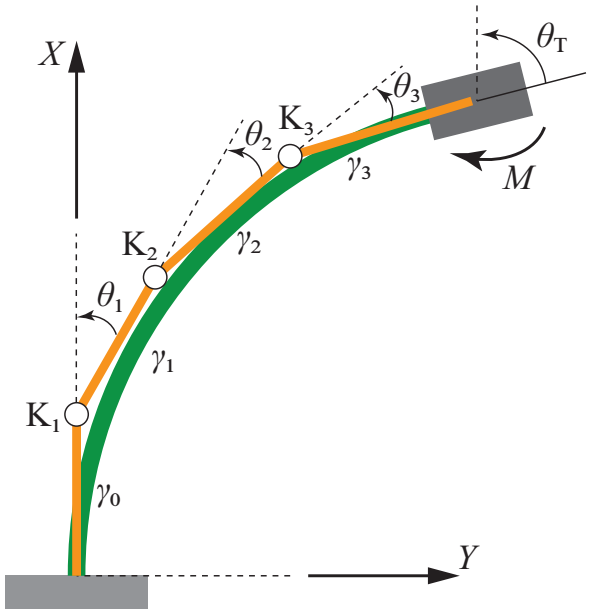

Fig. 3: A cantilever beam (green) deflected by a bending moment at its tip, and its 3R pseudo-rigid-body model (yellow). The flexible beam is replaced with rigid links connected by revolute joints and torsion springs.

IV. Magnetic Actuation

In this section, the actuation system used to control the catheter is described in brief, followed by calculation of the steering torque from the magnetic field, and calibration of the PRB model.

A. Actuation system

In this work, steering of the magnetic stenting catheter is demonstrated using a system with six mobile electromagnets called BigMag [17]. By controlling the positions of the electromagnets and the currents running through them, a desired magnetic field can be generated at any given point in the workspace. BigMag has a spherical workspace of 10cm diameter, which is sufficient to demonstrate proof-of-concept for clinical application. It can generate fields up to 60mT at a

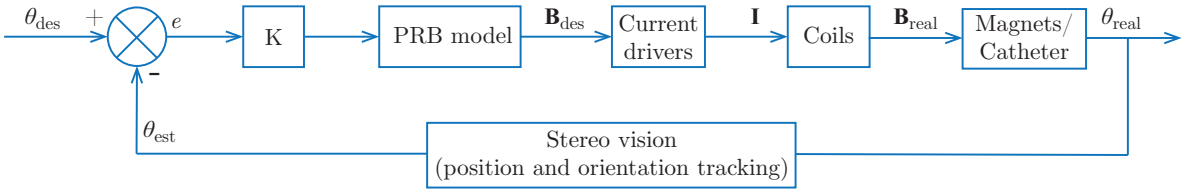

Fig. 4: Control loop for the catheter's tip bending angle. The desired orientation of the catheter tip (θ_{des}) is used to calculate the desired magnetic field ($\mathbf{B}_{des}$). The current drivers calculate the currents to be supplied to the coils, which produce the magnetic field ($\mathbf{B}_{real}$) that deflects the magnets on the catheter. The stereo vision setup is used to track the position and subsequently the orientation (θ_{est}) of the magnets to complete the control loop.

rate of 10Hz. The system has two built-in cameras that allow visualization from the top and the side. For the catheter steering experiments, a blood vessel replica with three branches is made from transparent polyvinylchloride (PVC) of 20 cm inner diameter, which is roughly the same size as the abdominal aorta. A motorized linear stage is used to insert and retract the catheter during experiments.

B. Magnetic field calculation

The magnetic field generated by BigMag is given by the superposition of the magnetic field generated by each individual electromagnetic coil.

$$\mathbf{B}(\mathbf{p}) = \sum_{i=1}^{6} \beta_i(\mathbf{p}, \theta)\ I_i\ , \tag{9}$$

where $\mathbf{B}$ is the magnetic field at point $\mathbf{p}$ in the workspace, $\beta_i(\mathbf{p}, \theta)$ represents the mapping from current I_i in i^{th} coil to the field generated by it at $\mathbf{p}$, with θ defining the system configuration at that instant of time. For details about the magnetic field generation, see Ref. [17].

The steering of the magnetic catheter is achieved using magnetic torques. A magnet with a dipole moment (μ) in a magnetic field ($\mathbf{B}$) experiences a torque (τ_B) that tries to align the magnet to the direction of external field.

$$\tau_B = \mu \times \mathbf{B}\ . \tag{10}$$

The magnetic torque acts on the magnets attached to the catheter, causing it to bend. The magnetic field can be varied in order to achieve different bends in the catheter tip to steer it along a blood vessel.

C. Catheter steering

In order to steer the catheter along the blood vessel, the position and orientation of the catheter tip must be controlled during catheter insertion and removal. To this end, the closed-loop control scheme shown in Fig. 4 is implemented. The controller uses the 3R PRB model to convert the user input (in this case, the desired catheter tip deflection) to a magnetic torque and subsequently, a magnetic field. The field mapping is used to calculate the currents necessary to generate the required field, leading to deflection of the catheter tip. The camera images are used to calculate the actual deflection of the catheter, and the error between the desired and actual values is fed through a gain K.

A graphical user interface (GUI) is developed to aid the catheter steering in BigMag (Fig. 5). It allows the user to choose the desired position and orientation of the tip magnet, while allowing visualization of the catheter using camera images. The user can control the catheter insertion with ease, while the magnetic field calculations using the control loop are moved to the background. The field values and the position and orientation of the catheter tip are still available in the GUI for clarity.

V. Results

In this section, the functioning of the magnetic stenting catheter is demonstrated through experiments . The steerability of the catheter is demonstrated first, followed by angiography and angioplasty functions.

The steering of the catheter using magnetic fields is illustrated in Figs. 6 and 7. In Fig. 6, the inner catheter (without the balloon sheath) is steered through two branches of the Y-shaped blood vessel phantom in the vertical plane. The insertion and retraction of the catheter is done using the linear stage. In Fig. 7, the branches are in the horizontal plane. In both cases, it is noticeable that the catheter tip does not push against the wall of the vessel since the catheter tip can be bent using the magnetic field. It is observed from experiments that the addition of second more proximal magnet enhances this behavior by facilitating a smooth bend of the catheter tip. This limits the chance of perforation, which is a benefit of magnetic catheterization.

The angiography function is demonstrated through an experiment in a tank of water (Fig. 8). The Y-shaped phantom is placed in the tank of water, the catheter is inserted into it. A hand-held permanent magnet is used to steer the catheter tip into one of the branches of the phantom. The proximal end of the catheter is connected to a syringe with a brown-colored dye, which is then injected through the catheter. The dye is released through the tip of the catheter, but only into the branch where the catheter tip is positioned, demonstrating the potential for effective angiography using this design.

The stenting function is also demonstrated in the same phantom (Fig. 9). Once the catheter tip is positioned in one of the branches of the phantom using the hand-held magnet, the outer sheath with the balloon and a stent is inserted over the inner catheter. When the stent is in place, the balloon is inflated, causing the stent to expand and attach to the walls of the vessel. The balloon is then deflated and the catheter retracted, leaving the stent in place. For the demonstration here, the stent is made from acrylonitrile butadiene styrene (ABS), and is fabricated by 3D printing.

VI. Conclusions and Future Work

This paper presents the design of a stenting catheter for cardiovascular applications that can be steered using magnetic

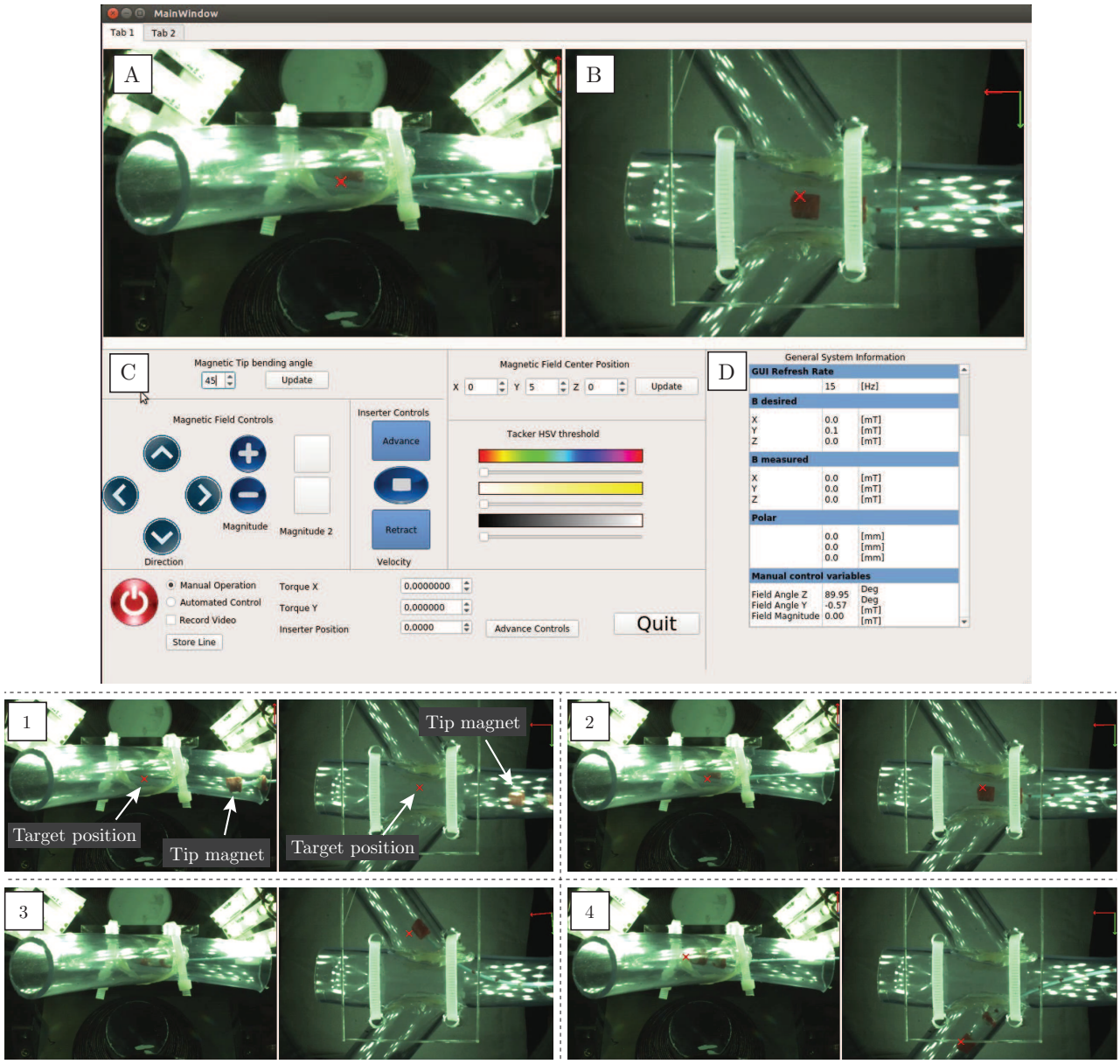

Fig. 5: (Top) The Graphical User Interface (GUI) for magnetic steering of the catheter. (A-B) The side and top views of the setup. (C) Panel for controlling the orientation of the catheter tip. (D) Feedback of controller data. (Bottom) Sequence of images (1-4) demonstrating catheter tip being guided to various target positions.

fields. The developed prototype uses two magnets near the tip in order to achieve smooth bends that minimize the chance of vessel perforation during catheterization. The steering of the catheter tip is demonstrated using an electromagnetic actuation system through a user-friendly GUI. Other necessary functions such as dye release for angiography and multiple stenting for complex angioplasties are also demonstrated. All experiments are performed in a replica of an abdominal aorta, aiming for minimally invasive treatment of AAA.

In this work, the magnetic steering is demonstrated using a laboratory setup of six mobile electromagnets, but it can also be accomplished using other clinical systems including existing commercial ones. Off-the-shelf components (magnets, catheter lumen, balloon) are used to fabricate the prototype, while they can be custom-made for specific application. This also means that the catheter can be sufficiently miniaturized for use in smaller blood vessels such as the coronary arteries. The visualization of the catheter and the blood vessels is done through camera images, but this can be replaced with X-ray images during clinical operation.

Future work will look at eliminating the need for fluoroscopic imaging and prevent exposure to radiation. This can be achieved by developing the catheter design to be compatible with magnetic resonance imaging (MRI), which is safe for humans. It is also possible to steer the catheter by utilizing the magnetic field of an MRI system. Tools for other surgical procedures (ablation, plaque removal, biopsy) will also be developed to fully exploit the benefits of magnetic actuation for minimally invasive cardiovascular surgery.

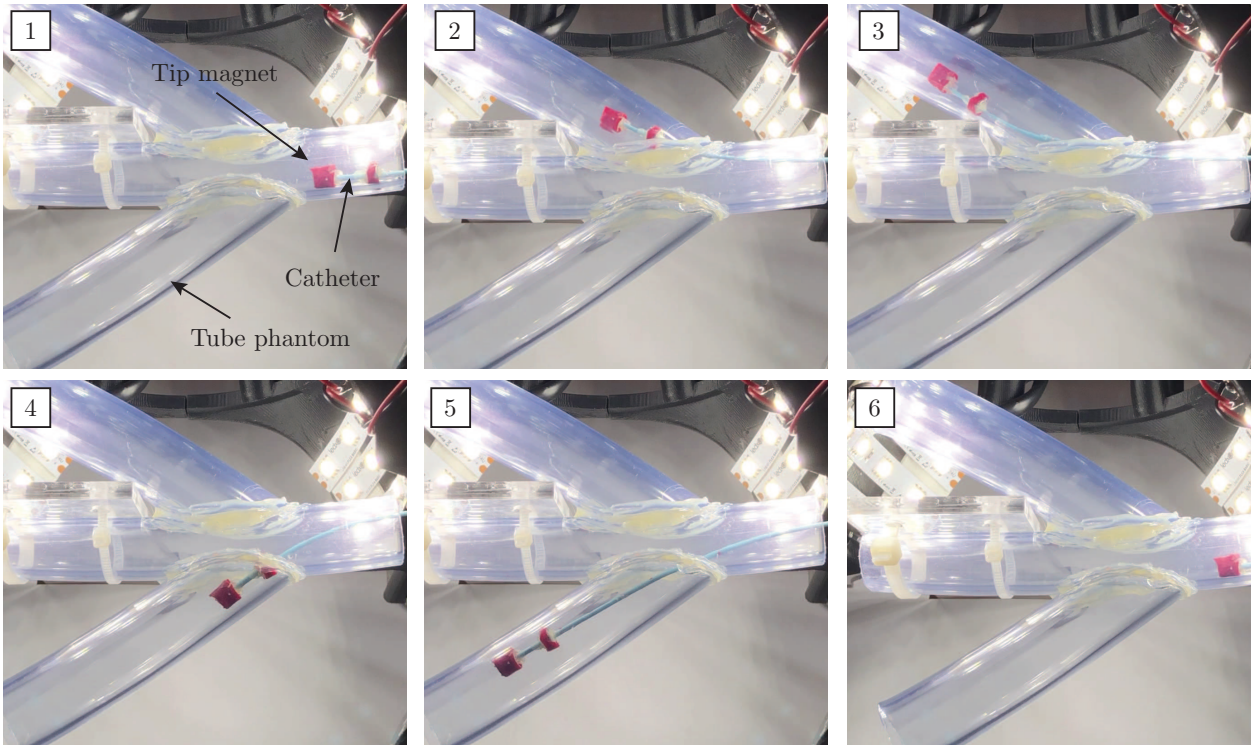

Fig. 6: Catheter steering in vertical plane. (1) The catheter is initially at the entry point of the phantom. (2-3) Steering into upper branch of phantom. (4-5) Steering into lower branch of phantom. (6) Retraction of catheter to entry point.

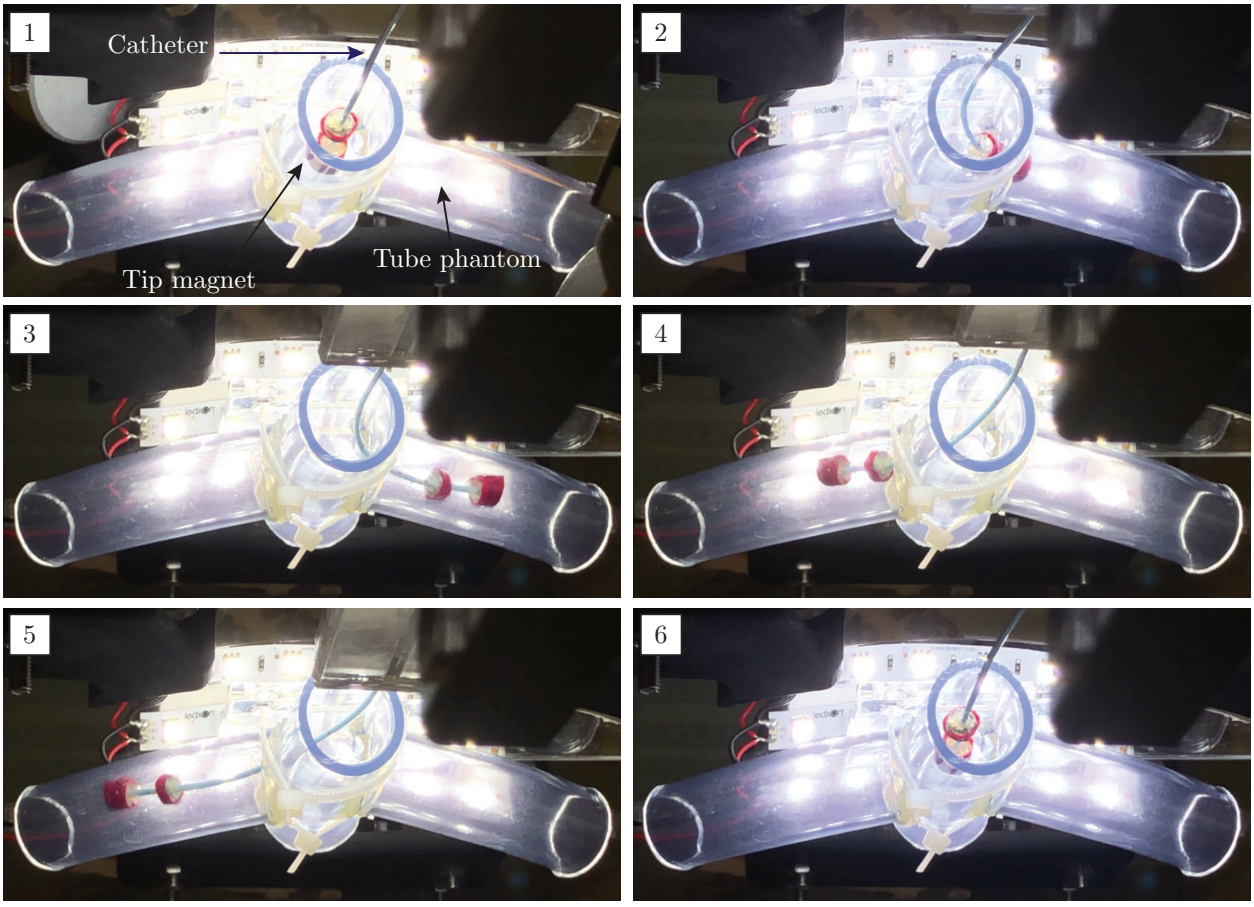

Fig. 7: Catheter steering in horizontal plane. (1) The catheter is initially at the entry point of the phantom. (2-3) Steering into right-sided branch of phantom. (4-5) Steering into left-sided branch of phantom. (6) Retraction of catheter to entry point.

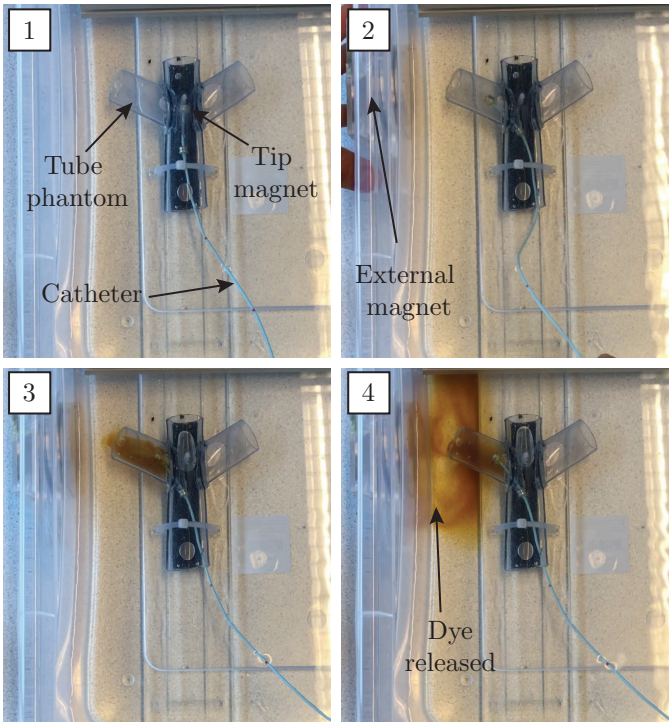

Fig. 8: Demonstration of angiography function using magnetic catheter in phantom filled with water. (1-2) Catheter is guided to target location using an external magnet. (3-4) Colored dying agent is released at target location through the dye channel of the catheter body.

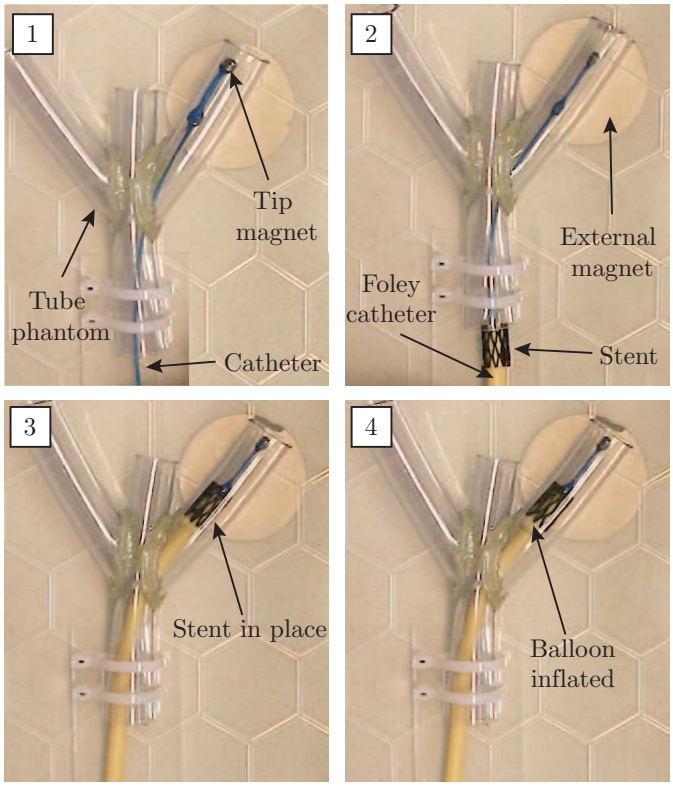

Fig. 9: Demonstration of angioplasty function using magnetic catheter. (1) Catheter tip is guided to and held at target location using an external magnet. (2) Foley catheter with a mock stent is inserted over the body of the magnetic catheter. (3-4) The stent reaches the target location, following which the balloon is inflated to deploy the stent.

REFERENCES

[1] World Health Organization, *World Health Statistics 2016: Monitoring Health for the SDGs Sustainable Development Goals*. World Health Organization, 2016.

[2] Z. J. Wanken, J. A. Barnes, S. W. Trooboff, J. A. Columbo, T. K. Jella, D. J. Kim, A. Khoshgowari, N. B. V. Riblet, and P. P. Goodney, "A Systematic Review and Meta-analysis of Long-term Reintervention after Endovascular Abdominal Aortic Aneurysm Repair," *Journal of Vascular Surgery*, vol. 72, no. 3, pp. 1122–1131, 2020.

[3] M. Mehrotra, J. R. D'Cruz, and M. E. Arthur, "Video-Assisted Thoracoscopy," in *StatPearls*. Treasure Island (FL): StatPearls Publishing, 2020.

[4] T. Doenst, M. Diab, C. Sponholz, M. Bauer, and G. Färber, "The Opportunities and Limitations of Minimally Invasive Cardiac Surgery," *Deutsches Ärzteblatt International*, vol. 114, no. 46, pp. 777–784, 2017.

[5] D. Daye and T. G. Walker, "Complications of endovascular aneurysm repair of the thoracic and abdominal aorta: evaluation and management," *Cardiovascular Diagnosis and Therapy*, vol. 8, no. Suppl 1, pp. S138–S156, 2018.

[6] M. L. Bloa, S. Abadir, K. Nair, B. Mondésert, and P. Khairy, "New Developments in Catheter Ablation for Patients with Congenital Heart Disease," *Expert Review of Cardiovascular Therapy*, pp. 1–12, 2020.

[7] F. Bessière, C. Zikry, L. Rivard, K. Dyrda, and P. Khairy, "Contact force with magnetic-guided catheter ablation," *EP Europace*, vol. 20, pp. ii1–ii4, 2018.

[8] L. Di Biasi, S. T. Fahmy, D. Patel, R. Bai, K. Civello, O. M. Wazni, M. Kanj, C. S. Elayi, C. K. Ching, M. Khan, L. Popova, R. A. Schweikert, J. E. Cummings, D. J. Burkhardt, D. O. Martin, M. Bhargava, T. Dresing, W. Saliba, M. Arruda, and A. Natale, "Remote Magnetic Navigation," *Journal of the American College of Cardiology*, vol. 50, no. 9, pp. 868–874, 2007.

[9] J. Bradfield, R. Tung, R. Mandapati, N. G. Boyle, and K. Shivkumar, "Catheter Ablation Utilizing Remote Magnetic Navigation: A Review of Applications and Outcomes," *Pacing and Clinical Electrophysiology*, vol. 35, no. 8, pp. 1021–1034, 2012.

[10] C. M. Heunis, J. Sikorski, and S. Misra, "Flexible Instruments for Endovascular Interventions: Improved Magnetic Steering, Actuation, and Image-Guided Surgical Instruments," *IEEE Robotics Automation Magazine*, vol. 25, no. 3, pp. 71–82, 2018.

[11] T. Liu, N. Lombard Poirot, T. Greigarn, and M. Cenk Çavuşoğlu, "Design of a Magnetic Resonance Imaging Guided Magnetically Actuated Steerable Catheter," *Journal of Medical Devices*, vol. 11, no. 2, pp. 0 210 041–2 100 411, 2017.

[12] J. Sikorski, E. S. A. A. M. Rutting, and S. Misra, "Grasping Using Magnetically-Actuated Tentacle Catheter: A Proof-of-Concept Study," in *2018 IEEE International Conference on Biomedical Robotics and Biomechatronics (Biorob)*, Aug. 2018, pp. 609–614.

[13] S. Jeon, A. K. Hoshiar, K. Kim, S. Lee, E. Kim, S. Lee, J.-y. Kim, B. J. Nelson, H.-J. Cha, B.-J. Yi, and H. Choi, "A Magnetically Controlled Soft Microrobot Steering a Guidewire in a Three-Dimensional Phantom Vascular Network," *Soft Robotics*, Oct. 2018.

[14] Y. Kim, G. A. Parada, S. Liu, and X. Zhao, "Ferromagnetic Soft Continuum Robots," *Science Robotics*, vol. 4, no. 33, 2019.

[15] A. Azizi, C. C. Tremblay, K. Gagné, and S. Martel, "Using the Fringe Field of a Clinical MRI Scanner Enables Robotic Navigation of Tethered Instruments in Deeper Vascular Regions," *Science Robotics*, vol. 4, no. 36, 2019.

[16] J. C. Norton, P. R. Slawinski, H. S. Lay, J. W. Martin, B. F. Cox, G. Cummins, M. P. Y. Desmulliez, R. E. Clutton, K. L. Obstein, S. Cochran, and P. Valdastri, "Intelligent Magnetic Manipulation for Gastrointestinal Ultrasound," *Science Robotics*, vol. 4, no. 31, 2019.

[17] J. Sikorski, I. Dawson, A. Denasi, E. E. G. Hekman, and S. Misra, "Introducing BigMag - A Novel System for 3D Magnetic Actuation of Flexible Surgical Manipulators," in *2017 IEEE International Conference on Robotics and Automation (ICRA)*, May 2017, pp. 3594–3599.

[18] V. K. Venkiteswaran, J. Sikorski, and S. Misra, "Shape and Contact Force Estimation of Continuum Manipulators using Pseudo-rigid-body Models," *Mechanism and Machine Theory*, vol. 139, pp. 34–45, 2019.

[19] V. K. Venkiteswaran and H.-J. Su, "A Versatile 3R Pseudo-Rigid-Body Model for Initially Curved and Straight Compliant Beams of Uniform Cross Section," *Journal of Mechanical Design*, vol. 140, no. 9, pp. 092 305–092 305–8, 2018.